ACS APPLIED MATERIALS & INTERFACES

Research Article

www.acsami.org

# Significantly Improved Luminescence Properties of Nitrogen-Polar (000$\bar{1}$) InGaN Multiple Quantum Wells Grown by Pulsed Metalorganic Chemical Vapor Deposition

Jie Song,*[,†] Shih-Pang Chang,[†,‡] Cheng Zhang,[†] Ta-Cheng Hsu,[§] and Jung Han[†]

[†]Department of Electrical Engineering, Yale University, New Haven, Connecticut 06520, United States

[‡]Department of Electro-Optical Engineering, National Chiao Tung University, 1001 Ta Hsueh Road, Hsinchu, Taiwan 300, Republic of China

[§]R&D Division, Epistar Co., Ltd., Science-based Industrial Park, Hsinchu, Taiwan 300, Republic of China

Supporting Information

**ABSTRACT:** We have demonstrated nitrogen-polar (000$\bar{1}$) (N-polar) InGaN multiple quantum wells (MQWs) with significantly improved luminescence properties prepared by pulsed metalorganic chemical vapor deposition. During the growth of InGaN quantum wells, Ga and N sources are alternately injected into the reactor to alter the surface stoichiometry. The influence of flow duration in pulsed growth mode on the luminescence properties has been studied. We find that use of pulsed-mode creates a high density of hexagonal mounds with an increased InGaN growth rate and enhanced In composition around screw-type dislocations, resulting in remarkably improved luminescence properties. The mechanism of enhanced luminescence caused by the hexagonal mounds is discussed. Luminescence properties of N-polar InGaN MQWs grown with short pulse durations have been significantly improved in comparison with a sample grown by a conventional continuous growth method.

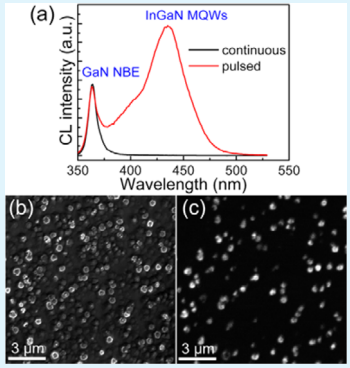


**KEYWORDS:** *N-polar, InGaN MQWs, MOCVD, photoluminescence, mounds*

## INTRODUCTION

III-Nitride semiconductors benefit from their direct and tunable bandgaps, and are the backbone for short-wavelength optoelectronics as well as high power and high frequency electronic devices. Currently, the majority of commercial III-nitrides optoelectronic and electronic devices are prepared on gallium-polar (0001) (Ga-polar) oriented templates. In comparison with the Ga-polar orientation, the reversed direction of the polarization-induced electric field in nitrogen-polar (000$\bar{1}$) (N-polar) heterostructures allows for the exploration of new device designs and is especially attractive for applications such as AlGaN/GaN high electron mobility transistors and high performance light emitting diodes (LEDs). For instance, in AlGaN/GaN heterojunction field-effect transistors, the location of the two-dimensional electron gas can be altered by switching from the Ga- to N-polar orientation to achieve enhanced electrical properties.[1,2] Simulation and experimental results suggest that the reversed polarization-induced electric field in N-polar LEDs and laser diodes would have a reduced efficiency droop and a lower threshold current density, respectively, with a suppression of electron overflow and the resulting increase in injection efficiency.[3,4] It was also found that N-polar LEDs are expected to benefit from polarization-enhanced dopant activation with a higher concentration of holes and improved carrier injection mechanism. In addition, with a nitrogen-rich surface atomic configuration, InGaN multiple quantum wells (MQWs) grown N-polar GaN is expected to have an enhanced incorporation of indium,[5] an important consideration in making high efficiency long wavelength visible LEDs possible. Growth of N-polar GaN with smooth surfaces and comparable crystalline quality as Ga-polar GaN has been demonstrated using off-cut substrates.[6,7] Many efforts have also been put into growing N-polar MQWs or LEDs in order to achieve high performance. However, so far, the luminescence properties of N-polar MQWs or LEDs reported are rather poor, ~20 to 100 times weaker than those of Ga-polar MQWs or LEDs.[5,8,9] Speculative reasons include a higher density of microstructural defects and native point defects, or the presence of impurities in N-polar InGaN quantum wells (QWs) such as C and O.[8,9]

In this work, we have demonstrated a noncontinuous, flow-modulated growth technique, named pulsed-mode, to grow N-polar MQWs with significantly improved luminescence properties. During the growth of InGaN QWs, Ga and N sources are alternately injected into the reactor to enhance the surface migration of adatoms and also alter the surface stoichiometry for facilitating the surface kinetics. The influence of flow durations in pulsed growth mode on the luminescence

Received: September 9, 2014
Accepted: December 11, 2014
Published: December 11, 2014

  

properties has been studied, and it shows that the MQWs sample grown with short duration exhibits brighter luminescence. Further investigation shows that under pulsed growth mode, the InGaN QWs surface creates many hexagonal mounds with enhanced In composition and increased thickness of InGaN QWs around screw-type dislocations, thus improving the luminescence properties by enhancing the localization of carriers and quantum dot-like enhanced emission at the mounds. Luminescence properties of N-polar InGaN MQWs grown with short pulse durations have been dramatically enhanced in comparison with the sample grown by a conventional continuous growth method, named continuous-mode. Our work provides a useful approach for preparing high brightness N-polar MQWs and LEDs.

## EXPERIMENTAL SECTION

Prior to the growth of InGaN MQWs, N-polar GaN epilayers used as templates were grown on c-plane (0001) sapphire with 2° off-cut toward the A-axis according to the procedure reported earlier.[6,10] Sapphire was heated up for nitridation in a mixture of ammonia ($NH_3$) (3 slm) and $N_2$ (4 slm) in a horizontal metalorganic chemical vapor deposition (MOCVD) reactor to 950 °C for 30 s. A 20 nm GaN nucleation layer was then grown on nitridized sapphire at 600 °C in $H_2$ carrier gas, followed by growing 1 $\mu$m N-polar GaN at 1055 °C and 100 mbar, with a $NH_3$ flow rate of 0.5 slm and a trimethylgallium (TMGa) flow of 66 $\mu$mol/min. During the growth, TMGa and $NH_3$ were used as Ga and N sources, respectively. The surface of the N-polar GaN template is very smooth and featureless under optical microscopy. The N-polarity of GaN templates was confirmed by convergent beam electron diffraction and wet etching in KOH solution.[6,10] After growth of N-polar GaN templates, the temperature was ramped down to 830 °C to grow five pairs of InGaN MQWs under $N_2$ carrier gas. Triethylgallium (TEGa), trimethylindium (TMIn) and $NH_3$ were used as Ga, In and N sources, respectively. During the growth of MQWs, a pulsed-mode was employed to grow InGaN quantum wells (QWs), whereas continuous-mode was used to grow GaN quantum barriers (QBs). Details about the flow pattern of pulsed-mode will be discussed later.

After growth, room temperature (RT) photoluminescence (PL) was conducted to examine the luminescence properties using a 325 nm He−Cd laser with laser power and beam size of ~8 mW and 1 $mm^2$, respectively. Temperature dependent PL was performed using a 405 nm diode laser with an excitation power and beam size of 10 mW and 0.1 $mm^2$, respectively. To identify the origin of emission in microscale, the luminescence properties were also examined by cathodeluminescence (CL) and monochromatic CL mapping conducted at RT on a commercial MonoCL3 of Gatan and a JEOL JSM-6700F instrument operating at an acceleration voltage of 5 keV. Microscopic morphology was performed by a Nomarski optical microscope and a Hitachi SU-70 scanning electron microscopy (SEM) instrument. Microstructural properties were characterized by transmission electron microscopy (TEM) with a FEI F20 microscope operating at an acceleration voltage of 200 kV. TEM specimens were prepared by focused ion beam.

## RESULTS AND DISCUSSION

Pulsed growth mode allows us not only to enhance the surface migration of adatoms but also to vary the surface stoichiometry for facilitating the surface kinetics. Pulsed-mode can be conducted with different sequence patterns of flows of species. In our work, on the basis of the consideration of low surface migration of Ga adatoms at low temperature for growing InGaN QWs, we alternately pulsed Ga and N sources, while keeping the flow of In source constant because the surface migration of In adatoms is much higher than that of Ga adatoms at the typical growth temperature of InGaN MQWs. A schematic illustration of the temporal sequences of valves operation is shown in Figure 1. During the growth, the TEGa

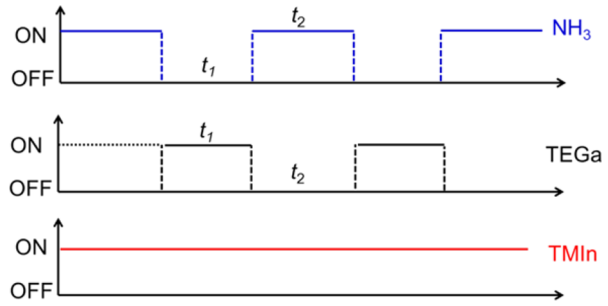


**Figure 1.** Schematic illustration of the temporal sequences of valves operation.

(black line) and $NH_3$ (blue line) sources were switched ON/OFF alternately, while TMIn (red line) was continuously injected at a constant flow rate. The durations of TEGa ON ($NH_3$ OFF) and TEGa OFF ($NH_3$ ON) are defined as $t_1$ and $t_2$, respectively. A reference sample was also prepared with the same structure but using continuous-mode to grow QWs for comparison.

In general, the durations of precursors switching "ON" and "OFF" are very important in pulsed growth mode. Many groups have conducted the pulsed growth mode for different purposes and have conducted investigations on the effect of pulse durations, such as the ability to influence the impurities incorporation rate in growing high quality GaAs,[11] lateral/vertical growth rate ratio in epitaxial lateral overgrowth,[12,13] the aspect ratio of GaN nanorods,[14] and so on. To get a sense about the effect of pulse durations on the properties of N-polar MQWs, here we first studied the influence of duration $t_1$ and $t_2$ on the properties of N-polar MQWs.

Figure 2 shows the RT PL spectra of N-polar MQWs samples grown in pulsed-mode with different $t_1$ values while

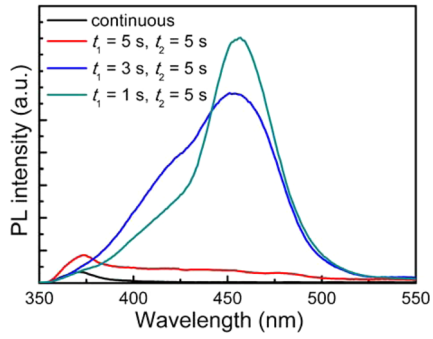


**Figure 2.** RT PL spectra of N-polar MQWs samples grown in pulsed-mode with different $t_1$ while keeping $t_2$ at 5 s, together with the continuously grown sample as the reference.

keeping $t_2$ at 5 s. As a comparison, we also show the PL spectrum of the sample grown in a conventional continuous mode (black curve). As seen in Figure 2, the PL of the sample grown in continuous-mode is very poor, with only one clearly visible peak of GaN near band emission (NBE) at 365 nm, similar to the results reported by other groups.[8,9,15] As reported in the literature, Lai et al.[15] and Chèze et al.[9] did not obtain clearly visible emission peak from N-polar InGaN MQWs at RT. Keller et al.[5] and Masui et al.[8] reported much poorer


dx.doi.org/10.1021/am506162z | ACS Appl. Mater. Interfaces 2015, 7, 273−278

emission from N-polar MQWs in comparison with that from Ga-polar MQWs at RT. Akyol et al.[4,16] demonstrated N-polar LEDs grown on free-standing bulk GaN substrates with visible emission, but they did not report the comparison between N-polar and Ga-polar LEDs. After the pulsed growth mode was employed, the MQWs sample grown with both $t_1$ and $t_2$ of 5 s, does not show obvious improvement compared with the sample grown in continuous-mode. However, when $t_1$ is decreased to 3 s, the PL intensity exhibits a significant improvement with a new strong peak appearing at about 450 nm in addition to the GaN NBE. By decreasing $t_1$ further to 1 s, PL intensity continues to increase by another 1.3 times.

The surface morphologies of the samples grown with different $t_1$ values were examined by SEM. Figure 3b,c,d

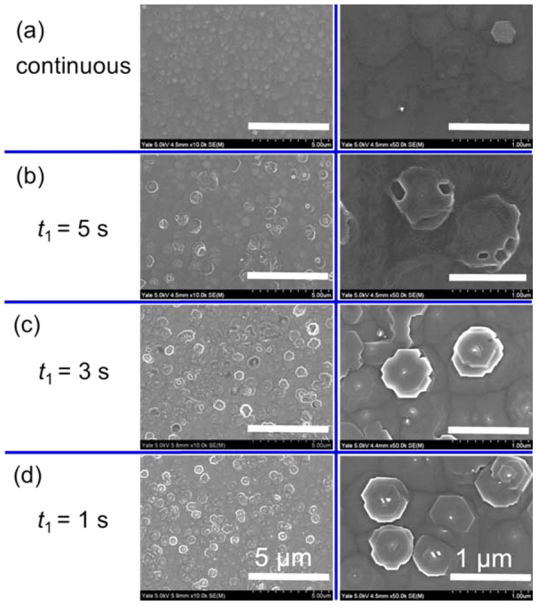


**Figure 3.** Top-view SEM images of N-polar MQWs samples grown in pulsed-mode with different $t_1$ while keeping $t_2$ at 5 s, together with the continuously grown sample as the reference. (a) Continuous-mode, (b) $t_1$ = 5 s, (c) $t_1$ = 3 s and (d) $t_1$ = 1 s.

shows the top-view SEM images of the samples grown with $t_1$ values of 5, 3 and 1 s, respectively, while keeping $t_2$ at 5 s, together with the continuously grown sample as the reference (Figure 3a). The left and right columns of Figure 3 show SEM images taken under low and high magnification, respectively. The surface of sample grown in continuous-mode has many tiny hillocks due to the low surface mobility of absorbed species on N-polar surface under $N_2$ carrier gas, consistent with the results reported by Keller et al.[5] However, we find that the surface of sample grown in pulsed-mode shows high density of hexagonal islands (here called "mounds") with diameter of about 300−500 nm in addition to the tiny hillocks. The density of these mounds increases with decreasing $t_1$, while the size of mounds changes very little. More detailed information about the mounds was also obtained by atomic force microscopy (AFM) and cross-sectional SEM, shown in Figures S1 and S2, respectively, in the Supporting Information. The density of the mounds is found to increase with decreasing $t_1$, exhibiting a similar trend as the PL intensity on the dependence of $t_1$. This indicates that there may be a correlation between the enhanced PL intensity and the mounds.

Figure 4 shows the RT PL spectra of N-polar MQWs samples grown with different $t_2$ while keeping $t_1$ at 3 s. The RT

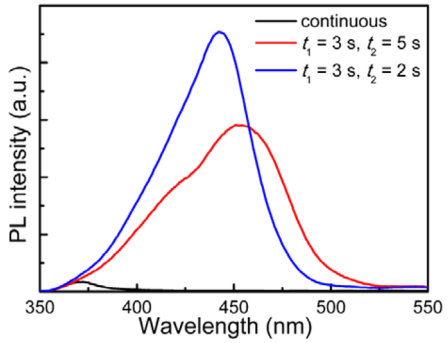


**Figure 4.** RT PL spectra of N-polar MQWs sample grown in pulsed growth mode with different duration $t_2$ while keeping $t_1$ at 3 s, together with the continuously grown sample as the reference.

PL spectrum of continuously grown sample is also shown as the reference. As shown in Figure 4, PL intensity of the sample grown in pulsed-mode increases gradually with decreasing $t_2$, with a strong peak appearing at ∼450 nm. The sample grown with $t_1$ and $t_2$ of 3 and 2 s, respectively, exhibits a dramatic improvement compared with the sample grown in continuous-mode.

The surface morphologies of the samples grown with different durations of $t_2$ were also examined by SEM. Figure 5 shows the top-view SEM images of N-polar MQWs samples

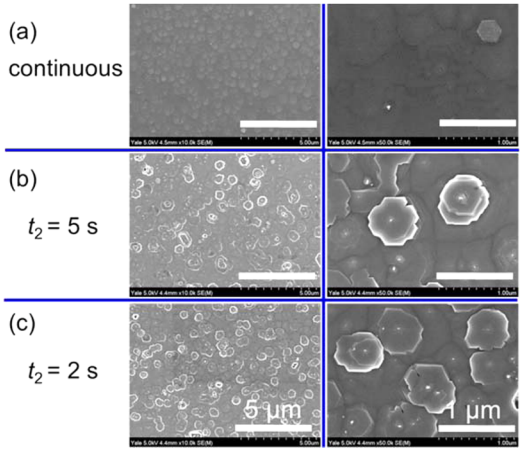


**Figure 5.** Top-view SEM images of N-polar MQWs samples grown with different $t_2$ values while keeping $t_1$ at 3 s, together with the continuously grown sample as the reference. (a) Continuous-mode, (b) $t_2$ = 5 s and (c) $t_2$ = 2 s.

grown with $t_2$ values of 5 and 2 s, while keeping $t_1$ at 3 s, together with the continuously grown sample as the reference. The density of hexagonal mounds on the surface increases with decreasing $t_2$, showing a similar trend as the PL intensity. This indicates again that the enhancement of the PL intensity may be caused by these mounds.

To understand the correlation between the mounds and the enhanced PL intensity, we studied the growth evolution of N-polar MQWs with varying the number of QWs. Figure 6 shows the PL spectra of N-polar MQWs samples grown with an increasing number of QWs from 1 to 10. $t_1$ and $t_2$ for this set of experiments are kept at 3 and 5 s, respectively. The intensity of


dx.doi.org/10.1021/am506162z | ACS Appl. Mater. Interfaces 2015, 7, 273−278

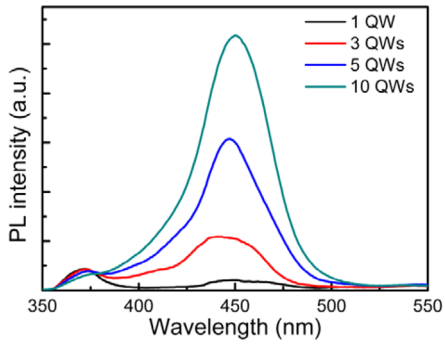


**Figure 6.** PL spectra of the samples grown with different numbers of QWs.

PL peak at 450 nm increases gradually by increasing the number of QWs. The top-view SEM images of these samples grown with different number of QWs are shown in Figure 7 in

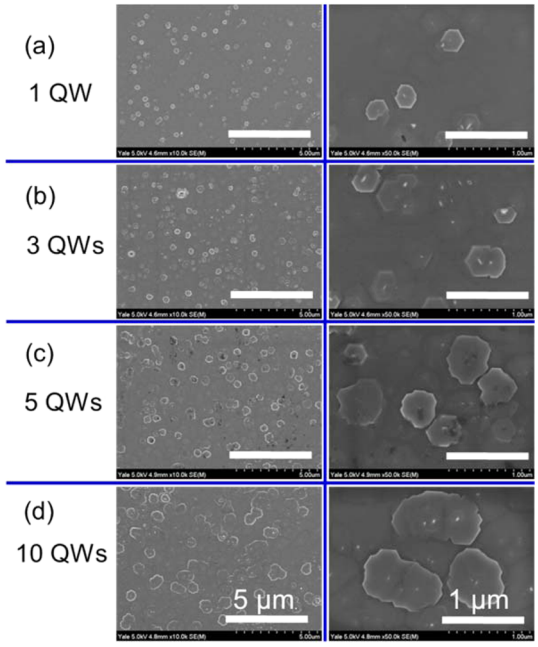


**Figure 7.** Top-view SEM images of the samples grown with QW numbers of (a) 1, (b) 3, (c) 5 and (d) 10.

the same format as Figure 3. It is found that the density of mounds increases dramatically with increasing number of QWs from 1 to 3, and then nearly saturates when the number of QWs exceeds 5. However, we observe that the size of mounds increases monotonically with increasing the number of QWs. We interpret that the enhanced PL intensity cannot be simply due to the increase of density of mounds, but relates to the increase of total area of mounds. The dependence of integrated PL intensity on the area ratio of mounds is shown in Figure S3 in the Supporting Information. It shows that integrated PL intensity increases almost linearly with respect to the area ratio of mounds on the surface.

To further understand the mechanism of enhanced luminescence properties of N-polar MQWs grown in pulsed-mode, we examined the correlation between mounds and enhanced luminescence by CL. Figure 8a shows the RT CL spectra of MQWs samples grown in continuous-mode (black curve) and pulsed-mode (red curve) with $t_1$ and $t_2$ values of 3

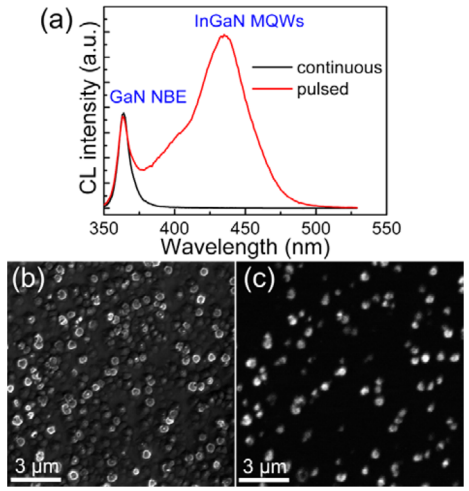


**Figure 8.** (a) CL spectra of N-polar MQWs sample grown in continuous-mode (black curve) and pulsed-mode (red curve). (b) Top-view SEM image of sample grown in pulsed-mode. (c) Monochromatic CL mapping collected at a wavelength of 440 nm from the identical sample region as that in panel b.

and 2 s, respectively. The sample grown in continuous-mode does not exhibit any visible CL in the range of 400−500 nm, except for the GaN NBE emission at 365 nm, as shown by the black curve in Figure 8a. However, the sample grown in pulsed-mode exhibits a distinct emission peak at around 440 nm, as shown by red curve, consistent with the PL results shown in Figure 4. A SEM image of the corresponding CL scanning area on the sample grown in pulsed-mode is presented in Figure 8b, and many hexagonal mounds are observed on the surface. Monochromatic CL mapping was collected at a wavelength of 440 nm from the same sample region and the map is shown in Figure 8c. A strong correlation is observed between the mounds shown in the SEM image and the bright spots from the monochromatic CL map. This suggests that the enhanced CL intensity is caused by the segregation of InGaN associated with the formation of mounds in pulsed growth mode.

To investigate the mechanism of the formation of mounds, cross-sectional TEM was conducted on the sample grown in pulsed-mode for further understanding the microstructural property. Figure 9a,b shows the bright-field cross-sectional TEM images of same region taken under two beam condition with **g** vectors of ⟨0002⟩ and ⟨11$\bar{2}$0⟩, respectively, and with zone axis of [1$\bar{1}$00]. Screw-, edge- and mixed-types of threading dislocations are labeled as s, e and m, respectively. The mound is marked by a red dashed rectangle. According to the TEM images in Figure 9a,b, we find that the mounds seem to be formed at the apexes of dislocations with screw-type component, including pure screw-type and mixed-type dislocations. We did not observe any mounds at the apexes of pure-edge type dislocations over the entire TEM specimen region. It has been reported that In/Ga adatoms prefer to nucleate at the apexes of screw-type dislocations because of the spiral atomic steps generated at screw-type dislocations,[17,18] resulting in increased growth rate of InGaN and enhanced In incorporation rate at the apexes of screw-type dislocations.[19] Enhanced growth rate of InGaN is also confirmed by the zoomed-in cross-sectional TEM imaging. Figure 9c shows the bright field cross-sectional TEM image with a high magnification about the edge of mounds and the InGaN QWs are labeled by white lines. It shows that the first InGaN QW grown at the


dx.doi.org/10.1021/am506162z | ACS Appl. Mater. Interfaces 2015, 7, 273−278

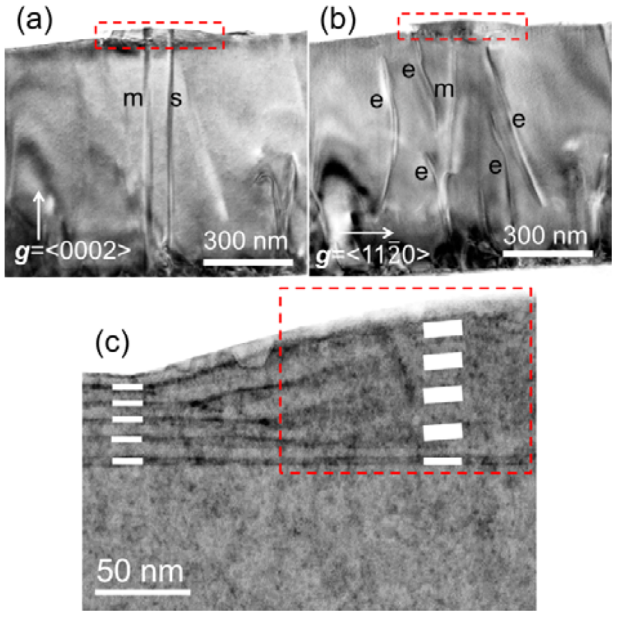


**Figure 9.** Bright field cross-sectional TEM images taken with **g** vectors of (a) ⟨0002⟩ and (b) ⟨11$\bar{2}$0⟩. (c) Cross-sectional TEM image at the region of the edge of mound with high magnification. The InGaN QWs are indicated by white short lines.

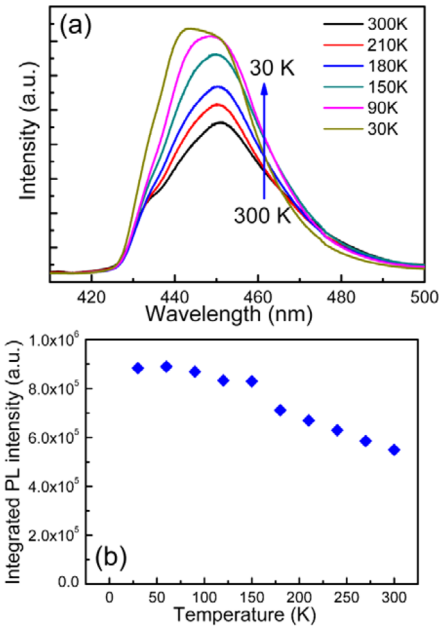


**Figure 10.** (a) PL spectra measured at different temperatures of the samples grown in pulsed-mode. (b) Integrated intensity between 420 and 500 nm of the samples grown in pulsed-mode.

mound has a similar thickness as the QWs grown on the flat region. However, starting from the second InGaN QW, the QWs become much thicker in the mound compared with the QWs in the flat region. The mounds with higher In composition and thicker QWs generate the emission at ∼440 nm. The enhanced luminescence can be interpreted by the following reasons. First, mounds with higher In composition enhance the localization of carriers and increase the radiative recombination ratio, thus resulting in an improved luminescence property. Second, the locally thicker QWs in the mounds may be characterized by a weaker internal electrical field, thus increasing the luminescence in mounds.[20] Similar results have been reported in quantum dots and quantum wires.[21−23] Therefore, the MQWs sample with higher density and thicker mounds exhibits stronger luminescence. The decrease of both $t_1$ and $t_2$ will increase the chance to form higher density of clusters of In/Ga atoms nucleating at the apexes of screw-type dislocations, eventually leading to enhanced PL intensity with decreasing both $t_1$ and $t_2$.

Low temperature PL measurement was conducted to further determine the luminescence properties of N-polar MQWs. Figure 10a shows the PL spectra of N-polar MQWs grown in pulsed-mode ($t_1$ = 3 s and $t_2$ = 2 s) measured at different temperatures. It is clear that the PL intensity increases with decreasing temperature. The emission peak of InGaN MQWs does not exhibit a pronounced S-shaped peak shift pattern probably because of the broad emission.[8] The integrated PL intensity between 420 and 500 nm is also plotted in Figure 10b as the function of temperature. The integrated PL intensity increases by a factor of ∼2 with decreasing the temperature from 300 to 30 K.

## CONCLUSION

In conclusion, we have investigated the growth of N-polar MQWs by employing a pulsed-mode growth scheme to improve the luminescence properties. The influence of the pulse durations and growth evolution have been studied, and it is found that short pulse durations play an important role in creating hexagonal mounds on the surface and enhancing the PL intensity. By further investigation with CL and TEM, we find that the mounds are formed around screw-type dislocations, giving strong emission with increased In composition. PL intensity of the sample grown in pulsed-mode has been enhanced significantly in comparison with the sample grown in continuous-mode. Our work suggests a useful approach for preparing high brightness N-polar MQWs and LEDs.

## ASSOCIATED CONTENT

### Supporting Information

Surface morphologies examined by AFM of InGaN MQWs grown in pulsed-mode (Figure S1), cross-sectional SEM image of mounds and plan-view SEM image of InGaN MQWs surface morphology after KOH etching (Figure S2), and dependences of area ratio of mounds and integrated PL intensity on the number of QWs (Figure S3). This material is available free of charge via the Internet at http://pubs.acs.org.

## AUTHOR INFORMATION

### Corresponding Author

*J. Song. Phone: (203)432-4302. Fax: (203)432-7769. E-mail: jiesong132@gmail.com.

### Notes

The authors declare no competing financial interest.

## ACKNOWLEDGMENTS

We acknowledge research support from Epistar Corp. and use of facilities supported by Yale Institute for Nanoscience and Quantum Engineering and NSF MRSEC DMR 1119826.

## REFERENCES

(1) Keller, S.; Suh, C. S.; Chen, Z.; Chu, R.; Rajan, S.; Fichtenbaum, N. A.; Furukawa, M.; DenBaars, S. P.; Speck, J. S.; Mishra, U. K.

Properties of N-Polar AlGaN/GaN Heterostructures and Field Effect Transistors Grown by Metalorganic Chemical Vapor Deposition. *J. Appl. Phys.* **2008**, *103*, 033708-1−003708-4.
(2) Wong, M. H.; Pei, Y.; Palacios, T.; Shen, L.; Chakraborty, A.; McCarthy, L. S.; Keller, S.; DenBaars, S. P.; Speck, J. S.; Mishra, U. K. Low Nonalloyed Ohmic Contact Resistance to Nitride High Electron Mobility Transistors Using N-Face Growth. *Appl. Phys. Lett.* **2007**, *91*, 232103-1−232103-3.
(3) Yen, S.-H.; Kuo, Y.-K. Polarization-Dependent Optical Characteristics of Violet InGaN Laser Diodes. *J. Appl. Phys.* **2008**, *103*, 103115-1−103115-6.
(4) Akyol, F.; Nath, D. N.; Krishnamoorthy, S.; Park, P. S.; Rajan, S. Suppression of Electron Overflow and Efficiency Droop in N-Polar GaN Green Light Emitting Diodes. *Appl. Phys. Lett.* **2012**, *100*, 111118-1−111118-4.
(5) Keller, S.; Fichtenbaum, N. A.; Furukawa, M.; Speck, J. S.; DenBaars, S. P.; Mishra, U. K. Growth and Characterization of N-Polar InGaN/GaN Multiquantum Wells. *Appl. Phys. Lett.* **2007**, *90*, 191908-1−191908-3.
(6) Sun, Q.; Cho, Y. S.; Lee, I.-H.; Han, J.; Kong, B. H.; Cho, H. K. Nitrogen-Polar GaN Growth Evolution on C-plane Sapphire. *Appl. Phys. Lett.* **2008**, *93*, 131912-1−131912-3.
(7) Keller, S.; Fichtenbaum, N. A.; Wu, F.; Brown, D.; Rosales, A.; DenBaars, S. P.; Speck, J. S.; Mishra, U. K. Influence of the Substrate Misorientation on the Properties of N-Polar GaN films Grown by Metal Organic Chemical Vapor Deposition. *J. Appl. Phys.* **2007**, *102*, 083546-1−083546-6.
(8) Masui, H.; Keller, S.; Fellows, N.; Fichtenbaum, N. A.; Furukawa, M.; Nakamura, S.; Mishra, U. K.; DenBaars, S. P. Luminescence Characteristics of N-Polar GaN and InGaN Films Grown by Metal Organic Chemical Vapor Deposition. *Jpn. J. Appl. Phys.* **2009**, *48*, 071003-1−071003-5.
(9) Chèze, C.; Siekacz, M.; Muzioł, G.; Turski, H.; Grzanka, S.; Kryśko, M.; Weyher, J. L.; Boćkowski, M.; Hauswald, C.; Lähnemann, J.; Brandt, O.; Albrecht, M.; Skierbiszewski, C. Investigation on the Origin of Luminescence Quenching in N-Polar (In,Ga)N Multiple Quantum Wells. *J. Vac. Sci. Technol., B: Nanotechnol. Microelectron.: Mater., Process., Meas., Phenom.* **2013**, *31*, 03C130-1−03C130-7.
(10) Sun, Q.; Suk Cho, Y.; Kong, B. H.; Koun Cho, H.; Shine, K. T.; Yerino, C. D.; Lee, I.-H.; Han, J. N-Face GaN Growth on C-Plane Sapphire by Metalorganic Chemical Vapor Deposition. *J. Cryst. Growth* **2009**, *311*, 2948−2952.
(11) Mochizuki, K.; Ozeki, M.; Kodama, K.; Ohtsuka, N. Carbon Incorporation in GaAs Layer Grown by Atomic Layer Epitaxy. *J. Cryst. Growth* **1988**, *93*, 557−561.
(12) Zhang, X.; Dapkus, P. D.; Rich, D. H. Lateral Epitaxy Overgrowth of GaN with $NH_3$ Flow Rate Modulation. *Appl. Phys. Lett.* **2000**, *77*, 1496−1498.
(13) Fareed, R. S. Q.; Yang, J. W.; Zhang, J.; Adivarahan, V.; Chaturvedi, V.; Khan, M. A. Vertically Faceted Lateral Overgrowth of GaN on SiC with Conducting Buffer Layers Using Pulsed Metal-organic Chemical Vapor Deposition. *Appl. Phys. Lett.* **2000**, *77*, 2343−2345.
(14) Lin, Y.-T.; Yeh, T.-W.; Dapkus, P. D. Mechanism of Selective Area Growth of GaN Nanorods by Pulsed Mode Metalorganic Chemical Vapor Deposition. *Nanotechnology* **2012**, *23*, 465601-1−465601-6.
(15) Lai, Y.-L.; Liu, C.-P.; Lin, Y.-H.; Lin, R.-M.; Lyu, D.-Y.; Peng, Z.-X.; Lin, T.-Y. Effect of the Material Polarity on the Green Emission Properties of InGaN/GaN Multiple Quantum Wells. *Appl. Phys. Lett.* **2006**, *89*, 151906-1−151906-3.
(16) Akyol, F.; Nath, D. N.; Gür, E.; Park, P. S.; Rajan, S. N-Polar III-Nitride Green (540 nm) Light Emitting Diode. *Jpn. J. Appl. Phys.* **2011**, *50*, 052101-1−052101-3.
(17) Oliver, R. A.; Kappers, M. J.; Humphreys, C. J.; Briggs, G. A. D. Growth Modes in Heteroepitaxy of InGaN on GaN. *J. Appl. Phys.* **2005**, *97*, 013707-1−013707-8.
(18) Burton, W. K.; Cabrera, N.; Frank, F. C. The Growth of Crystals and the Equilibrium Structure of Their Surfaces. *Philos. Trans. R. Soc., A* **1951**, *243*, 299−358.
(19) Song, J.; Xu, F. J.; Yan, X. D.; Lin, F.; Huang, C. C.; You, L. P.; Yu, T. J.; Wang, X. Q.; Shen, B.; Wei, K.; Liu, X. Y. High Conductive Gate Leakage Current Channels Induced by In Segregation Around Screw- and Mixed-Type Threading Dislocations in Lattice-Matched $In_xAl_{1-x}N$/GaN Heterostructures. *Appl. Phys. Lett.* **2010**, *97*, 232106-1−232106-3.
(20) Keller, S.; Li, H.; Laurent, M.; Hu, Y.; Pfaff, N.; Lu, J.; Brown, D. F.; Fichtenbaum, N. A.; Speck, J. S.; DenBaars, S. P.; Mishra, U. K. Recent Progress in Metal-Organic Chemical Vapor Deposition (000$\bar{1}$) N-Polar Group-III Nitrides. *Semicond. Sci. Technol.* **2014**, *29*, 113001-1−113001-46.
(21) Lubyshev, D. I.; González-Borrero, P. P.; Marega, E., Jr.; Petitprez, E.; La Scala, N., Jr.; Basmaji, P. Exciton Localization and Temperature Stability in Self-Organized InAs Quantum Dots. *Appl. Phys. Lett.* **1996**, *68*, 205−207.
(22) Lee, J.-S.; Isshiki, H.; Sugano, T.; Aoyagi, Y. InGaAs/GaAs Quantum Nanostructure Fabrication on GaAs Vicinal Substrates by Atomic Layer Epitaxy. *J. Appl. Phys.* **1998**, *83*, 5525−5528.
(23) Saito, T.; Arakawa, Y. Electronic Structure of Piezoelectric $In_{0.2}Ga_{0.8}N$ Quantum Dots in GaN Calculated Using a Tight-Binding Method. *Phys. E* **2002**, *15*, 169−181.